Surg Radiol Anat (2013) 35:295–300
DOI 10.1007/s00276-012-1034-8

ORIGINAL ARTICLE

A comparison of subchondral bone mineralization between the glenoid cavity and the humeral head on 57 cadaverous shoulder joints

Marko Kraljević · Valentin Zumstein · Rolf Hügli · Magdalena Müller-Gerbl

Received: 6 July 2012 / Accepted: 19 October 2012 / Published online: 3 November 2012

Abstract
Purpose Mineralization distribution of the subchondral bone plate can be used as a marker for long-term stress distribution in diarthrodial joints. Severe injuries or pathological changes of the glenohumeral joint often end in osteoarthritis, where shoulder arthroplasty has become the treatment of choice. The computed tomography osteoabsorptiometry (CT-OAM) is a non-invasive method to determine the distribution of the mineralization of the subchondral bone plate in vivo, which is an important factor concerning the implantation of orthopedic endoprostheses. The aim of this study was to investigate the mineralization of both joint partners of the glenohumeral joint and to compare them with each other.
Methods The distribution of the mineralization of the subchondral bone plate of 57 shoulder specimens was determined by means of CT-OAM. To evaluate a correlation between age and localization of subchondral mineralization maxima, the Chi-square test correlation test was applied.
Results Forty-nine glenoid cavities (86 %) showed a bicentric mineralization distribution pattern with anterior and posterior maxima, only 8 glenoid cavities (14 %) revealed a monocentric mineralization pattern with anterior maxima. Forty-five humeral heads (79 %) showed a bicentric distribution pattern with anterior and posterior maxima, 12 humeral heads (21 %) could be classified as monocentric with a centro-posterior pronounced maximum.
Conclusions We could demonstrate that stress distribution in both joint partners of the glenohumeral joint is inhomogeneous and characteristically bicentric due to the physiological incongruity. Monocentric mineralization patterns can result as a cause of age-related loss of incongruity.

Keywords Mineralization · Subchondral bone · Glenoid cavity · Humeral head · CT-OAM · Shoulder arthroplasty

M. Kraljević (✉) · V. Zumstein · M. Müller-Gerbl
Anatomical Institute, University of Basel, Pestalozzistrasse 20, 4056 Basel, Switzerland
e-mail: marko.kraljevic@gmail.com

R. Hügli
Institute of Radiology and Nuclear Medicine, Kantonsspital Bruderholz, 4101 Bruderholz, Switzerland

Introduction

The evolutionary transfer from quadrupedalism to bipedalism initiated the development of the upper limbs to a highly specialized gripping and sensing organ. The glenohumeral joint became a very important function related to the positioning of the hand in space. Severe injuries or pathological changes may limit this function and often characterize the beginning of a history of suffering that frequently ends in osteoarthritis. In such cases, shoulder arthroplasty has become the treatment of choice. Therefore, preoperative information about stress distribution in the shoulder joint is recommendable to evaluate the risk of postoperative complications such as joint instability and glenoid loosening [12, 23, 26]. Early identified and operative fixed cases improve postoperative outcomes [5, 28]. On this account, the conditions in the glenohumeral joint and the resulting stress distribution in the glenoid cavity as well as the humeral head are of great importance.

Characteristic mineralization patterns of the subchondral bone plate typify the loading history on articular surfaces [14]. Some authors demonstrated that changes in stress

have a direct influence on morphological alterations [21, 29]. Relationships between long-term stress and subchondral bone were affirmed by later studies [6, 14, 20, 25]. Some authors discussed the age [18], the shape of a joint [25] and the geometry of the articular surface [2, 25] as important factors for the mineralization of the subchondral bone plate. The computed tomography osteoabsorptiometry (CT-OAM) is a non-invasive method to demonstrate the mineralization distribution in the subchondral bone plate of diarthrodial joints in vivo [14]. In contrast to the usual methods of CT densitometry, which deal with the calculation of an absolute value for bone density in a larger area including compact and cancellous bone, CT-OAM is a procedure for demonstrating differences in relative concentration within a joint surface and enables conclusions about low and highly loaded areas [19].

Mineralization patterns of the glenoid cavity and the humeral head have never been compared with one another before. Information about their morphological changes would contribute to the understanding of their interaction and the mechanical situation by the use of CT-OAM as a non-invasive method for in vivo assessment of individual long-term stress [14]. We hypothesized that the density patterns of the glenoid cavity correlate to the density patterns of the humeral head. The aim of this study was to determine the mineralization patterns of the glenoid cavity and the humeral head in macroscopically healthy shoulder specimens and to compare them with each other.

Materials and methods

Preparation

A total of 57 glenoid cavities and humeral heads of the Anatomical Institute of University of Basel and the Anatomical Institute of Ludwig Maximilian University in Munich were obtained. They were all fixated in formalin. The age distribution of the glenohumeral joints in this study was from 18 to 95 years (35 males, 22 females) with an average age of 61 years. The subjects consisted of the scapula, the clavicle, the proximal humerus and the surrounding tissue. After the soft tissue was dissected and removed, the joint capsule was opened and the glenohumeral joint disarticulated. Specimens with signs of degeneration or traumatic findings were excluded from our study.

Computed tomography osteoabsorptiometry

CT data sets, recorded in a GE Lightspeed 16 X-ray CT scanner (General Electric Healthcare Corporation, Waukesha, WI, USA) with a layer thickness of 0.6 mm in transverse slices, were used to demonstrate the mineralization [14–17]. Data obtained were edited using the image analyzing system ANALYZE 7.5.5. (Biomedical Imaging Resource, Mayo Foundation, Rochester, MN, USA). First a three-dimensional reconstruction was generated and then registered in a frontal view. In a next processing step, the subchondral bone plate was sliced and isolated and reconstructed in 3D using a maximum intensity projection, where the values with the highest density are projected onto the surface. Then, the gray values of the subchondral bone plate were converted to false colors. The density range from <200 to >1,200 HU was divided into gray value stages of 100 HU each. Black typified density values over 1,200 HU, followed in descending order by red, orange, yellow, green and blue. Overlaying the cavity and the humeral head with the false color figure resulted in the topographical view of mineralization patterns (Fig. 1). The resulting images served as a basis for further evaluation.

The densitograms of glenoid cavity and the humeral head were analyzed in a standardized procedure. To quantify the distribution patterns, a 21 × 30 unit grid with identical sectors (IU) was projected onto the densitogram of each cavity. A 21 × 21 unit grid was used for the humeral head. The grid was positioned in tangential contact so that its borders matched the borders of the articular surface. The number of units was also kept the same, in order to standardize the coordinates for larger and smaller endplates. The coordinates of each mineralization maximum were selected to generate a summary image. We defined the maximum as an area of the two highest density levels compared with the surrounding subchondral bone.

Statistical analysis

To examine differences between the mineralization patterns, groups of corresponding maxima were built visually and compared by use of mean values and standard deviations. Statistical analysis of these data was performed with the Chi-square test. The level of significance was <0.05.

Results

The subchondral mineralization distribution revealed two dissimilar types of density patterns. In 49 glenoid cavities (86 % of 57 specimens), we found a bicentric distribution pattern with anterior and posterior maxima, concentrated in squares 4 and 6 (Fig. 2a). The localization of the anterior and posterior maximum was determined by the coordinates x_1/y_1 and x_2/y_2. The mean value for the anterior maximum was x_1 16.8 IU (SD 1.6 IU), y_1 18.3 IU (SD 2.7 IU), for the posterior maximum x_2 4.9 IU (SD 2.5 IU), y_2 17.3 IU (SD 3.4 IU) (Table 1). The mean age of the bicentric group was

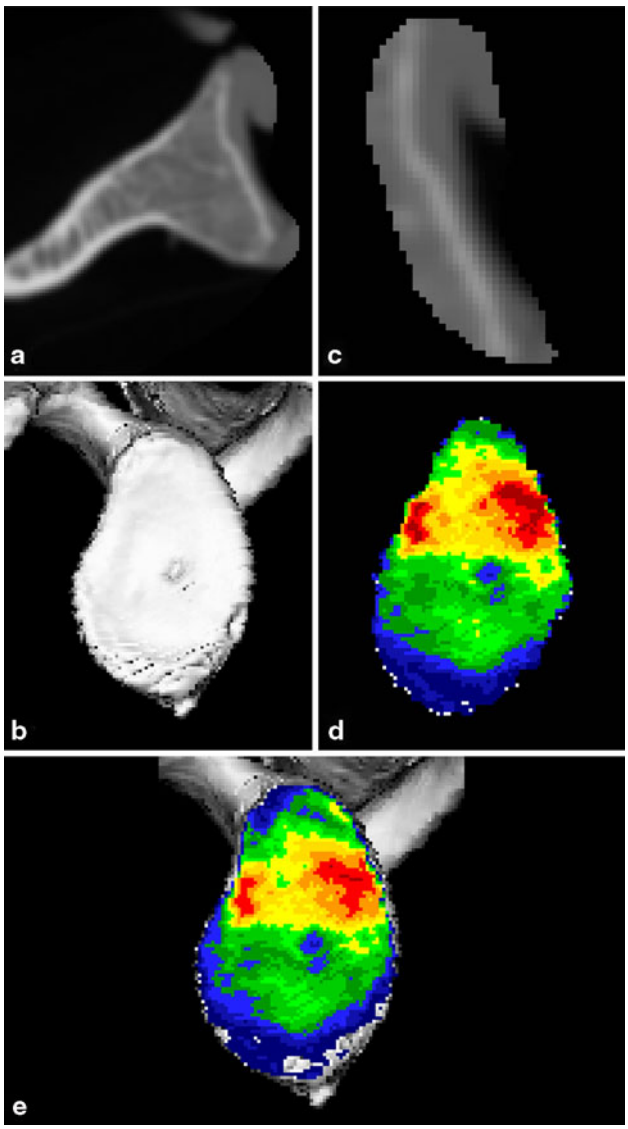

Fig. 1 Procedure of CT-OAM: **a** reconstruction of the articular surface, **b** three-dimensional reconstruction of the glenoid cavity, **c** isolation of the subchondral bone plate, **d** reconstruction of the subchondral bone plate by means of maximum intensity projection, **e** full view of the finished densitogram

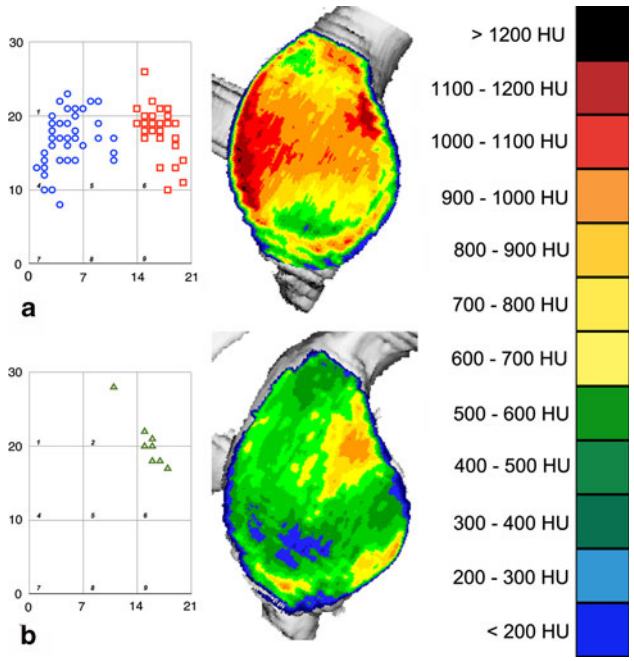

Fig. 2 Summary chart of all maxima in **a** bicentric and **b** monocentric glenoid cavities (anterior is on the *right*, posterior is on the *left*) compared with a typical example of the mineralization distribution

Table 1 Localization of the maxima within the joint surface of the glenoid cavity and the humeral head

	Glenoid cavity		Humeral head	
	Mean (IU)	SD (IU)	Mean (IU)	SD (IU)
x_1	16.8	1.6	4.9	1.5
y_1	18.3	2.7	12.7	3.2
x_2	4.9	2.5	16.1	1.2
y_2	17.3	3.4	13.7	1.8
x_3	15.5	2.1	13.4	4.3
y_3	20.5	3.5	12.4	3.3

61 years (SD 25 years). Only 8 glenoid cavities (14 % of 57 specimens) revealed a monocentric mineralization pattern with anterior maxima (Fig. 2b). The localization of the maximum was determined by the coordinates x_3/y_3. The mean value for the anterior maximum was x_3 15.5 IU (SD 2.1 IU), y_3 20.5 IU (SD 3.5 IU). The mean age of the monocentric group was 66 years (SD 20 years).

Forty-five humeral heads (79 % of 57 specimens) showed a bicentric distribution pattern with anterior and posterior maxima, concentrated in squares 4 and 6 (Fig. 3a). The localization of the anterior and posterior maximum was determined by the coordinates x_1/y_1 and x_2/y_2. The mean value for the anterior maximum was x_1 4.9 IU (SD 1.5 IU), y_1 12.7 IU (SD 3.2 IU), for the posterior maximum x_2 16.1 IU (SD 1.2 IU), y_2 13.7 IU (SD 1.8 IU) (Table 1). The mean age of the bicentric group was 60 years (SD 25 years). Twelve humeral heads (21 % of 57 specimens) could be classified as monocentric with a centro-posterior pronounced maximum (Fig. 3b). The localization of the maximum was determined by the coordinates x_3/y_3. The mean value was x_3 13.6 IU (SD 4.2 IU), y_3 12.4 IU (SD 3.3 IU). The mean age of the monocentric group was 68 years (SD 21 years).

The correlation of the mineralization distribution patterns of the glenoid cavity and the humeral head revealed a high significance ($P < 0.001$). No statistically significant differences in the average age between bicentric and monocentric groups were found.

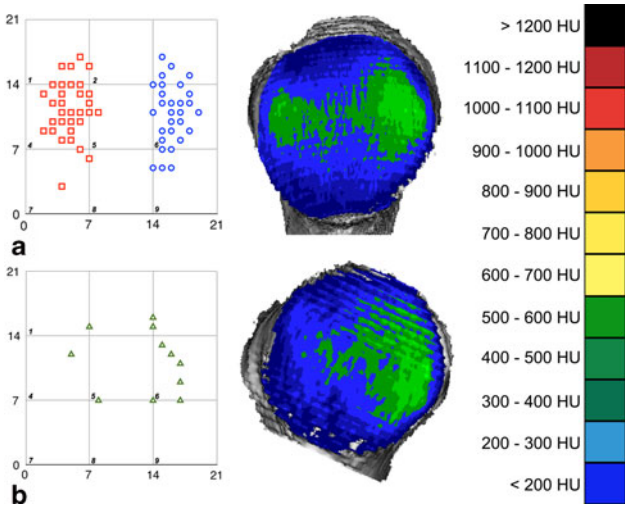

Fig. 3 Visualization of the maxima in all **a** bicentric and **b** monocentric humeral heads (anterior is on the *left*, posterior is on the *right*) compared with a typical example of the mineralization distribution

Discussion

In this study, we have investigated the relationship between the mineralization patterns of the glenoid cavity and the humeral head. The mineralization of the subchondral bone plate represents the long-term stress in diarthrodial joints [3, 14]. Geometry of the joint, age, side and the individual functional demands are all factors that affect the mineralization pattern of the subchondral bone plate [2, 6, 18, 20, 25]. It was shown that the density values of the subchondral mineralization are higher in younger individuals and athletes compared to older specimens [18]. A high level of muscle mass and individual exposure may be possible reasons for this situation [14, 18]. Two density maxima were found ventrally and dorsally in young patients whereas older patients showed a centrally located maximum [18]. Some authors stated that the vessel density was significantly higher in heavily loaded joints and stressed regions of the same joint [9, 11]. There is an existing interrelation between hand domination and the degree of absolute mineralization [22]. Some authors showed the impact of pathological situations on the subchondral mineralization patterns. For example, superiorly decentered mineralization patterns of the subchondral bone plate are typical for cuff arthropathies [24, 27]. This means that pathological conditions have an effect on the long-term stress and therefore on the mineralization of the subchondral bone plate. This underlines the importance of an early preoperative identification of such cases, to fix subluxation tendencies intraoperatively and improve postoperative results. The quantification of the mineralization by CT-OAM, which is based on conventional CT data set, could be a method for preoperative identification and postoperative follow-up. The CT-OAM is a reproducible and highly sensitive method to determine the subchondral bone mineralization in vitro and in vivo as well [14, 15]. In contrast to the usual methods of CT densitometry, which deal with the calculation of an absolute value for bone density, CT-OAM is a procedure for demonstrating differences in relative concentration within a joint surface [14].

Our intention was to investigate and compare the mineralization patterns of both joint partners in the glenohumeral joint, which has never been done so far. The examinations of the subchondral articular surfaces of the glenoid cavity and the humeral head showed regional differences in distribution of density and the position of maxima. We could find two characteristic mineralization patterns for the glenoid cavity as well as the humeral head. These distribution patterns in the subchondral bone plate of the glenoid cavity and the humeral head were confirmed in previous studies [22, 30].

Our summary chart of bicentric maxima (Fig. 4a) demonstrated the compliance between the glenoid cavity and the humeral head. The evaluation of the mean values and the statistical analysis, which reveals a highly significant correlation ($P < 0.001$), confirmed these findings. The bicentric distribution patterns of the glenoid cavity and the humeral head occur due to the physiological incongruity of the joint partners as a principle of physiological stress distribution to prevent osteoarthritis [1, 8, 14, 16, 22]. The tendency to a bigger humeral head than the respective glenoid cavity, which underlines this concept of physiological mismatch, was illustrated by means of stereophotogrammetry [24]. Furthermore, the articular cartilage is important for glenohumeral congruity. The swelling of the articular cartilage after periods of high loading increases incongruity and stimulates the cartilage to keep healthy which leads to concentrated contact in the anterior and posterior parts of the articular surface of both joint partners. This principle of incongruity in the glenohumeral joint causes bicentric mineralization patterns of the subchondral bone plate of the glenoid cavity and the humeral head as well and was confirmed through our testing. Age-related changes [14, 18] may modify the subchondral bone mineralization. We found no statistically significant differences in the average age between bicentric and monocentric for the glenoid cavity as well as the humeral head.

The monocentric distribution patterns, which occur less frequent than bicentric distribution patterns, may be caused by loss of incongruity with increasing age [14, 18]. They could potentially also represent the beginning of pathological changes such as cuff arthropathies [15, 22]. In these situations, where the infraspinatus muscle and the teres minor muscle are dominant, the humeral head is ventrally decentered. On this account, the posterior part of the glenoid cavity is in no contact with the humeral head. The

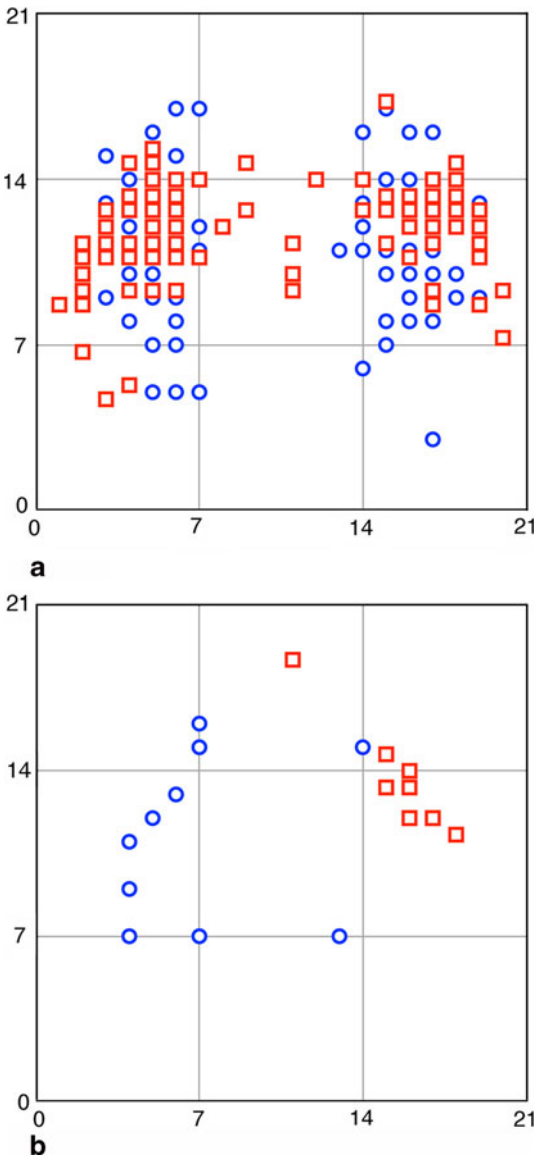

Fig. 4 Comparative summary chart of all **a** bicentric and **b** monocentric glenoid cavities (*squares*) and humeral heads (*circles*)

glenoid contact area is limited to the anterior part. On the other hand, the contact area of the humeral head displaces to the posterior part. This phenomenon explains our results in the summary chart of the monocentric distribution patterns (Fig. 4b).

The mineralization distribution of both joint partners of the glenohumeral joint, which typifies the loading history, showed characteristic and reproducible patterns. Comparisons between the glenoid cavity and the humeral head revealed a good compliance. Bicentric maxima located near the anterior and posterior rim of the glenoid cavity, respectively, anterior and posterior region of the humeral head, were found in most cases. Monocentric maxima resulted only in about a fifth of all specimens.

Mineralization distribution of the subchondral bone plate, which can be investigated by means of CT-OAM, gives important information about the long-term stress within a joint surface [15]. The subchondral bone plate in the glenohumeral joint is also an important factor concerning the implantation of orthopedic endoprostheses. It was found that the mineralization of the subchondral bone correlates with the mechanical strength [10, 13, 31]. Some authors stated the importance of cancellous bone for screw positioning [4, 7]. Therefore, areas of high density could serve as anchoring locations to get optimal fixation for orthopedic implants in case of resurfacing. Furthermore, information about subchondral bone density might be interesting for osteosynthesis, when screws are to be anchored in case of open reduction and internal fixation. Our intention in this study was to investigate the mineralization patterns in healthy shoulders to provide reproducible results but it would be of clinical interest to explore the subchondral bone plate mineralization in arthritic shoulders in the future.

Conflict of interest The authors declare that they have no conflict of interest.

Ethical standards All experiments comply with the current laws of Switzerland.

References

1. Aitken GK, Bourne RB, Finlay JB, Rorabeck CH, Andreae PR (1985) Indentation stiffness of the cancellous bone in the distal human tibia. Clin Orthop Relat Res 201:264–270
2. Bullough PG (1981) The geometry of diarthrodial joints, its physiologic maintenance, and the possible significance of age-related changes in geometry-to-load distribution and the development of osteoarthritis. Clin Orthop Relat Res 156:61–66. doi:10.1097/00003086-198105000-00008
3. Carter DR, Fyhrie DP, Whalen RT (1987) Trabecular bone density and loading history: regulation of connective tissue biology by mechanical energy. J Biomech 20(8):785–794
4. Chapman JR, Harrington RM, Lee KM, Anderson PA, Tencer AF, Kowalski D (1996) Factors affecting the pullout strength of cancellous bone screws. J Biomech Eng 118(3):391–398
5. Collins D, Tencer A, Sidles J, Matsen F 3rd (1992) Edge displacement and deformation of glenoid components in response to eccentric loading. The effect of preparation of the glenoid bone. J Bone Joint Surg Am 74(4):501–507
6. Frost HM (1990) Skeletal structural adaptations to mechanical usage (SATMU): 2. Redefining Wolff's law: the remodeling problem. Anat Rec 226(4):414–422. doi:10.1002/ar.1092260403
7. Gordon KD, Duck TR, King GJ, Johnson JA (2003) Mechanical properties of subchondral cancellous bone of the radial head. J Orthop Trauma 17(4):285–289
8. Hofmann AA, Hammon DJ, Daniels AU (1991) Compressive strength mapping of femoral head trabecular bone. J Rehabil Res Dev 28(2):25–32
9. Imhof H, Sulzbacher I, Grampp S, Czerny C, Youssefzadeh S, Kainberger F (2000) Subchondral bone and cartilage disease: a rediscovered functional unit. Invest Radiol 35(10):581–588

10. Kraljevic M, Zumstein V, Wirz D, Hugli R, Muller-Gerbl M (2011) Mineralisation and mechanical strength of the glenoid cavity subchondral bone plate. Int Orthop. doi:10.1007/s00264-011-1308-5
11. Lane LB, Villacin A, Bullough PG (1977) The vascularity and remodelling of subchondral bone and calcified cartilage in adult human femoral and humeral heads. An age- and stress-related phenomenon. J Bone Joint Surg Br 59(3):272–278
12. Matsen FA, Lippitt SB, Sidles JA, Harryman DT (1994) Practical evaluation and management of the shoulder. WB Saunders, Philadelphia
13. Muhlhofer H, Ercan Y, Drews S, Matsuura M, Meissner J, Linsenmaier U, Putz R, Muller-Gerbl M (2009) Mineralisation and mechanical strength of the subchondral bone plate of the inferior tibial facies. Surg Radiol Anat 31(4):237–243. doi:10.1007/s00276-008-0430-6
14. Muller-Gerbl M (1998) The subchondral bone plate. Adv Anat Embryol Cell Biol 141(III-XI):1–134
15. Muller-Gerbl M, Putz R, Hodapp N, Schulte E, Wimmer B (1989) Computed tomography-osteoabsorptiometry for assessing the density distribution of subchondral bone as a measure of long-term mechanical adaptation in individual joints. Skeletal Radiol 18(7):507–512
16. Muller-Gerbl M, Putz R, Hodapp N, Schulte E, Wimmer B (1990) Demonstration of subchondral density pattern using CT-osteoabsorptiometry (CT-OAM) for the assessment of individual joint stress in live patients. Z Orthop Ihre Grenzgeb 128(2):128–133. doi:10.1055/s-2008-1039487
17. Muller-Gerbl M, Putz R, Kenn R (1992) Demonstration of subchondral bone density patterns by three-dimensional CT osteoabsorptiometry as a noninvasive method for in vivo assessment of individual long-term stresses in joints. J Bone Miner Res 7(Suppl 2):S411–S418. doi:10.1002/jbmr.5650071409
18. Muller-Gerbl M, Putz R, Kenn R (1993) Distribution pattern of subchondral mineralization in the glenoid cavity in normal subjects, athletes and patients. Z Orthop Ihre Grenzgeb 131(1):10–13. doi:10.1055/s-2008-1039896
19. Muller-Gerbl M, Weisser S, Linsenmeier U (2008) The distribution of mineral density in the cervical vertebral endplates. Eur Spine J 17(3):432–438. doi:10.1007/s00586-008-0601-5
20. Oberlander W (1973) The stress of the human hip joint. V. The distribution of bone density in the human acetabulum (author's transl). Z Anat Entwicklungsgesch 140(3):367–384. doi:10.1007/BF00525062
21. Pauwels F (1965) Eine Theorie über den Einfluss mechanischer Reize auf dei Differenzierung der Stützgewebe. Z Anat Entwicklungsgesch 121:478–515
22. Schulz CU, Pfahler M, Anetzberger HM, Becker CR, Muller-Gerbl M, Refior HJ (2002) The mineralization patterns at the subchondral bone plate of the glenoid cavity in healthy shoulders. J Shoulder Elbow Surg 11(2):174–181. doi:10.1067/mse.2002.121635
23. Skirving AP (1999) Total shoulder arthroplasty—current problems and possible solutions. J Orthop Sci 4(1):42–53. doi:10.1007/s007760050073
24. Soslowsky LJ, Flatow EL, Bigliani LU, Mow VC (1992) Articular geometry of the glenohumeral joint. Clin Orthop Relat Res 285:181–190
25. Tillmann B (1971) The stress of the human elbow joint. I. Functional morphology of the articular surfaces. Z Anat Entwicklungsgesch 134(3):328–342. doi:10.1007/BF00519919
26. Torchia ME, Cofield RH, Settergren CR (1997) Total shoulder arthroplasty with the Neer prosthesis: long-term results. J Should Elb Surg 6(6):495–505. doi:10.1016/S1058-2746(97)90081-1
27. von Eisenhart-Rothe R, Muller-Gerbl M, Wiedemann E, Englmeier KH, Graichen H (2008) Functional malcentering of the humeral head and asymmetric long-term stress on the glenoid: potential reasons for glenoid loosening in total shoulder arthroplasty. J Should Elb Surg 17(5):695–702. doi:10.1016/j.jse.2008.02.008
28. Walch G, Badet R, Boulahia A, Khoury A (1999) Morphologic study of the glenoid in primary glenohumeral osteoarthritis. J Arthroplast 14(6):756–760. doi:10.1016/S0883-5403(99)90232-2
29. Wolff J (1892) Das Gesetz der Transformation der Knochen. August Hirschwald Verlag, Berlin
30. Zumstein V, Kraljevic M, Huegli R, Muller-Gerbl M (2011) Mineralisation patterns in the subchondral bone plate of the humeral head. Surg Radiol Anat. doi:10.1007/s00276-011-0819-5
31. Zumstein V, Kraljevic M, Wirz D, Hugli R, Muller-Gerbl M (2012) Correlation between mineralization and mechanical strength of the subchondral bone plate of the humeral head. J Should Elb Surg 21(7):887–893. doi:10.1016/j.jse.2011.05.018